Colloid Polym Sci (2004) 282: 661–669
DOI 10.1007/s00396-003-1007-x

ORIGINAL CONTRIBUTION

Andrea M. Santos
Abdelhamid Elaïssari
José M. G. Martinho
Christian Pichot

Preparation and characterization of carboxylic-containing poly(methyl methacrylate) nanolatexes

Received: 21 May 2003
Accepted: 30 September 2003
Published online: 18 November 2003

A.M. Santos · J.M.G. Martinho
Centro de Química-Física Molecular,
Instituto Superior Técnico,
Av. Rovisco Pais 1, 1049-001
Lisboa, Portugal

A. Elaïssari · C. Pichot (✉)
Unité Mixte CNRS-bioMérieux,
UMR-2142, ENS Lyon,
46 allée d'Italie, Cedex 07, 69364
Lyon, France
Tel.: +33-0-472728513
Fax: +33-0-472728533

Abstract Poly(methyl methacrylate) (PMMA)-based latex particles bearing carboxylic groups at the surface were prepared via emulsion polymerization. The polymerization recipe and process were optimized in order to target monodisperse particles with diameters around 100 nm. The polymerizations were performed using 4,4′-azobis(4-cyanopentanoic) acid (ACPA) as initiator and sodium dodecyl sulphate (SDS) as surfactant. The polymerization conversion was determined by both gas chromatography and gravimetry. The final latexes were characterized with respect to particle size, size distribution, surface charge density, electrokinetic properties (i.e. electrophoretic mobility vs pH and ionic strength) and colloidal stability (i.e. coagulation rate constants vs pH and stability factor vs ionic strength).

Keywords Poly(methyl methacrylate) · Nanoparticles · Surface carboxylic groups · Electrokinetic behaviour · Colloidal stability

Introduction

Polymer colloids present an attractive and increasing interest in various domains, with relevance for the biomedical field [1]. For many years, polystyrene latexes with several sizes have been prepared and widely used as supports for diagnostic purposes. However, very few systematic studies have been devoted to the use of PMMA particles as colloidal supports, although these particles can offer some advantages due to the higher polarity of the polymer compared to polystyrene. The synthesis of PMMA latexes has long been reported mostly by free-radical polymerization in suspension [2], dispersion [3, 4], emulsion [5, 6] and microemulsion [7]. Among these heterogeneous free-radical polymerization procedures, the emulsion process proved to be the most appropriate and versatile method to produce small and monodisperse particles [8]. As methyl methacrylate has higher solubility in water than styrene, homogeneous and coagulative nucleation mechanisms are expected to occur for surfactant-free or low surfactant concentrations (i.e. below the CMC).

Since our interest is the preparation of a polymer colloid support to study the immobilization, conformation and dynamics of a protein (enzyme) by fluorescence, several requirements should be fulfilled: (i) the colloid should be transparent in the region of absorption of the intrinsic fluorophore (tryptophan) of the protein; (ii) monodisperse low-size particles are required to improve reproducibility and reduce the scattering power of the latexes; and (iii) the surface groups of the particles should be relatively stable to hydrolysis and allow the covalent grafting of the biological species.

Following these requirements we decided to prepare PMMA particles bearing carboxylic groups at the surface. A general synthetic procedure relies on the use of minor amounts of unsaturated carboxylic acids such as the acrylic or methacrylic acids. However, this procedure gives latex particles exhibiting a complex surface

morphology and undesired water-soluble polyelectrolytes [9]. In order to produce a smooth polymer–water interface bearing a single stable surface group (carboxylic acid), the latexes were prepared by emulsion polymerization using 4,4′-azobis(4-cyanopentanoic) acid (ACPA) as initiator and sodium dodecyl sulphate (SDS) as emulsifier. Such a surfactant was selected since its low CMC and its relatively good stabilizing efficacy allow the production of low-sized latexes. The particle size and size distribution were determined by dynamic light scattering and the final latex dispersions were characterized in terms of electrokinetic behaviour and colloidal stability. This work is part of a research programme devoted to the study of the immobilization of a recombinant enzyme (cutinase from *Fusarium solani pisi*) onto a model polymer colloid.

Experimental part

Materials

Methyl methacrylate (Aldrich, 99% pure) was purified by distillation under reduced pressure. The 4,4′-azobis (4-cyanopentanoic) acid initiator (Aldrich-Sigma, 75% pure) was recrystallized from a methanol/pentane mixture 1:1 (v/v). Sodium hydrogen carbonate (Merck, p.a.), Triton X-405, a polyethylene oxide nonylphenol ether with an average of 40 ethylene oxide (EO) units (Sigma, 70% pure) and sodium dodecyl sulphate (Fluka Chemika, p.a.) were used as received.

Preparation of PMMA nanospheres

A set of poly(methyl methacrylate) (PMMA) latexes were prepared by emulsion polymerization using methyl methacrylate (MMA), ACPA as initiator and Triton X-405 or SDS as surfactant. Two reactors of 50 and 250 mL equipped with a glass anchor-type stirrer running at 300 rpm, condenser and nitrogen inlet and outlet were used in the preliminary and further studies, respectively. The polymerizations were performed in an aqueous buffer solution (10^{-2} M $NaHCO_3$, pH 8.0–9.0) at constant temperature in the interval of 70–80 °C.

Polymerization kinetics

The polymerization kinetics was followed by gas chromatography (Perkin Elmer 9000 AutoSystem Gas Chromatograph) using an HP-1 capillary column and flame ionization detector. The samples were prepared by adding 50 μL of latex particles to 200 μL of an ethanol/toluene mixture (0.2% v/v in ethanol). Operating conditions were as follows: nitrogen flow rate 7.0 ml/min, oven temperature (50 °C), injection temperature (220 °C) and recording temperature (250 °C). After sample injection, its MMA content was determined from a calibration curve that was fitted by a linear expression according to Eq. 1,

$$A_{\mathrm{MMA}}/A_{\mathrm{toluene}} = 20.437 \times [\mathrm{MMA}] + 0.006; r^2 = 0.999 \quad (1)$$

where A_i are the peak areas of the chromatogram and [MMA] is the molar concentration of MMA monomer in the sample. The polymerization conversion, C, was then calculated using Eq. 2,

$$\%C = 100 \times \frac{\left(\frac{A_{\mathrm{MMA}}}{A_{\mathrm{toluene}}}\right)_{t_0} - \left(\frac{A_{\mathrm{MMA}}}{A_{\mathrm{toluene}}}\right)_{t}}{\left(\frac{A_{\mathrm{MMA}}}{A_{\mathrm{toluene}}}\right)_{t_0}} \quad (2)$$

where the index t refers to the polymerization time, t_0 being the initial time before adding the initiator. For comparison the overall conversions were also determined by gravimetry.

Particle characterization

The crude latex particles were cleaned by three cycles of centrifugation–redispersion using milli-Q water (deionized filtrated water) in order to remove the surfactant, oligomers and residual electrolytes. The conductivity of the serum decreased as a function of washing steps before reaching a value close to the conductivity of the used deionized water (~0.06 mS) after three cycles. The latex dispersions were characterized at room temperature (~23 °C) in terms of particle size, size distribution, morphology, electrophoretic mobility, surface charge density and colloidal stability.

Particle size and size distribution

The hydrodynamic diameter (D_p) and the polydispersity index (I_p) of the latex particles were obtained by quasi-elastic light scattering using both a Zetasizer (Malvern Instruments, 3000-HS model) and a light scattering apparatus (Brookhaven) equipped with a 35-mW He laser (Spectra Physics, model 127) and a BI-2030 AT autocorrelator. The morphology and size distribution of latex particles were also examined by scanning electron microscopy (Hitachi S2400). The samples were prepared by placing a drop of the dispersion (0.1% p/v in milli-Q water) directly onto a cold sample holder and drying at room temperature. All samples were sputtered with gold and analysed at a voltage of 10 kV.

Electrokinetic behaviour

The electrophoretic mobility (μ_e) of latex particles at several pH and ionic strengths was determined by a Zetasizer (Malvern Instruments, 3000-HS model). The pH was adjusted by adding HCl or NaOH to a solution of constant ionic strength (10^{-3}M NaCl). The salinity was varied between $10^{-5}$and 10^{-1} M NaCl at pH 6.

Colloidal stability

The colloidal stability of the latex dispersions was studied by turbidimetry ($\lambda = 350$ nm) using a UV–Vis spectrophotometer (Shimadzu UV-3101 PC). The turbidity was determined at several pH ~3–7 and constant ionic strength (10^{-2} M NaCl) and at pH 6 with varying ionic strength (0.03–0.08 M NaCl). The latexes were rapidly diluted in the desired medium, and the time evolution of the turbidity immediately recorded. The apparent coagulation rate constants, k_{coag}, were calculated as the initial slope of the optical density (OD) versus time t [10],

$$k_{\mathrm{coag}} = \frac{\partial OD}{\partial t}_{t=0} \quad (3)$$

The stability factor (W) was defined as the ratio of fast (k_f) to slow (k_s) coagulation rate constants,

$$W = \frac{k_f}{k_s} \quad (4)$$

Results and discussion

Preliminary studies

To synthesize monodisperse PMMA latexes with a particle size ~100 nm, various recipes (see Table 1) were investigated varying the surfactant (Triton X-405 and SDS), temperature, initiator (ACPA) and surfactant concentrations. Table 2 summarizes the results obtained for the overall polymerization conversion, C_p, and the characterization of the latexes in terms of size and polydispersity.

The first runs planned to study the effect of the initiator concentration (pmma§1 to pmma§3) for a constant amount of Triton X-405 (~3.5 CMC). By decreasing the initiator concentration the hydrodynamic particle size does not vary substantially, having a diameter around 107 nm. The desired particle size was reached, but unfortunately the size distribution was too high ($I_p = 0.13$ and 0.18), increasing with the concentration of initiator. This behaviour can in principle be attributed to the low stability of the formed particles during the nucleation step. Nevertheless, by increasing the amount of Triton X-405 (i.e. 4 CMC in pmma§4 and pmma§5 runs) the polydispersity index was not improved.

The broad size distribution can result from several sources: (i) the poor stabilizing effect of the Triton X-405 despite the high concentrations used; (ii) aggregation of the particles induced by a salt effect brought about by the ACPA; (iii) combination of both micellar and homogeneous/coagulative nucleation mechanisms during the polymerization, which could be favoured if the polyethylene oxide-based surfactant partitions between the organic and aqueous phases, as was shown before for Triton X-405 [11, 12]; and (iv) the presence of a steric and viscous layer formed by the adsorbed nonionic surfactant that decreases both the free radical entry and exit rate constants [13], favouring the aqueous media Creactions and hence perturbing the nucleation mechanism and its duration.

Suspecting that the main cause of the high polydispersity came from the poor stabilizing effect of the nonionic surfactant (Triton X-405), the next runs were made using an ionic surfactant, SDS. This time the temperature was decreased from 80 to 70 °C in order to slow down the decomposition rate of the initiator. The first run was performed at the CMC of SDS (pmma§6), and produced small particles (D_p~50 nm) with a better polydispersity. In order to increase particle size, the SDS concentration and the solid content were adjusted while maintaining the temperature and the amount of the initiator. The variation of the SDS concentration to 1/2 and 1/4 CMC (pmma§7 and pmma§8, respectively) resulted in an increase of particle diameter (D_p~63, 84 nm for pmma§7 and pmma§8, respectively). Finally, maintaining the SDS concentration equal to 1/4 CMC and increasing the solid content (pmma§9), the targeted particle size and size distribution were achieved.

Based on these preliminary results, a systematic study was performed focusing on the influence of SDS concentration on the polymerization kinetics.

Final results

Polymerization kinetics

Table 3 summarizes the recipes used for the preparation of the latex particles. In each recipe, the concentrations of initiator and MMA were maintained constant, while the concentration of SDS was varied below the CMC. Figure 1 shows the polymerization conversion curves

Table 2 Hydrodynamic particle diameter (D_p), and polydispersity index (I_p) and overall conversions (% C_p) for the PMMA latexes prepared in the preliminary studies

Latex	D_p /(nm)	I_p	% C_p
pmma_1	107	0.18	81.4
pmma_2	107.1	0.13	92.1
pmma_3	–	–	70.9
pmma_4	97.6	0.21	82.1
pmma_5	96.7	0.26	81.4
pmma_6	50.6	0.048	85.0
pmma_7	62.6	0.040	85.2
pmma_8	84.2	0.029	87.4
pmma_9	106.1	0.032	92.4

Table 1 Preliminary polymerization recipes

Latex	M_{H_2O} (g)	M_{ACPA}/ (g)	M_{MMA}/ (g)	M_{Triton}/ (g/100 g)	M_{SDS}/ (g/100 g)	T/ (°C)
pmma_1	55	0.050	2.5	0.32	0	80
pmma_2	55	0.025	2.5	0.33	0	80
pmma_3	55	0.012	2.5	0.33	0	80
pmma_4	55	0.013	2.5	0.38	0	80
pmma_5	55	0.025	2.5	0.38	0	80
pmma_6	55	0.051	2.5	0	0.121	70
pmma_7	55	0.051	2.5	0	0.066	70
pmma_8	55	0.051	2.5	0	0.033	70
pmma_9	55	0.051	5.0	0	0.034	70

Table 3 Latex recipes

Latex	M_{H_2O} (g)	M_{ACPA}/ (g)	M_{MMA}/ (g)	[SDS]/ (g/100 g)
pmma§1	250	0.208	21	0.0443
pmma§2	250	0.208	21	0.0550
pmma§3	250	0.208	21	0.0733
pmma§4	250	0.208	21	0.110
pmma§5	250	0.208	21	0.147

versus time followed by gravimetry and gas chromatography.

The polymerization was allowed to proceed up to a conversion of 90 or 95%, although a ~85% conversion was obtained for all runs after 30 min. The overall rate of emulsion polymerization R_p, when the main loci of polymerization are the swollen PMMA particles, is given by Eq. 5,

$$R_p = -\frac{d[M]}{dt} = k_p \frac{\tilde{n} N_p}{N_A} [M]_p \quad (5)$$

where k_p is the polymerization rate constant for the homogeneous reaction, N_p is the particle number density, $[M]_p$ is the concentration of monomer in the particles, N_A is the Avogadro number and $\tilde{n}$ is the average number of radicals per particle [14]. Knowing the polymerization rate constant, $k_p = 1050\ M^{-1}s^{-1}$ [15], the value of $\tilde{n}$ can be calculated from Eq. 5, since R_p is accessible from the experimental conversion curve and N_p from the mass of polymerized monomer and the particle size. Table 4 summarizes the overall polymerization rate (R_p), the particle number density (N_p) and average number of radicals per particle ($\tilde{n}$).

The increase of SDS concentration in the polymerization recipe enhances the initial polymerization rate by increasing the particle number and/or reducing the nucleation period. The average number of radicals per particle is much higher than 1/2 and decreases as SDS concentration increases. Such behaviour may be explained by the Trommsdorff effect considering pseudo-bulk conditions [16]. At higher conversions, the viscosity inside the particle increases and consequently the exit of the radicals from the particles is hindered. Then, the decrease of $\tilde{n}$ with the SDS concentration reflects the effect of the particle size on the number of radicals per particle.

Figure 2 shows the variation of the hydrodynamic particle size (R_h) with $\%C^{1/3}$. A straight line can be drawn through the experimental points, meaning that the particle number is constant during the polymerization, which corroborates the efficient stabilizing effect of the surfactant and the occurrence of a rapid nucleation.

Figure 3 shows the log–log plot of the particle number density versus the surfactant concentration, [SDS]. The experimental points follow the scaling law,

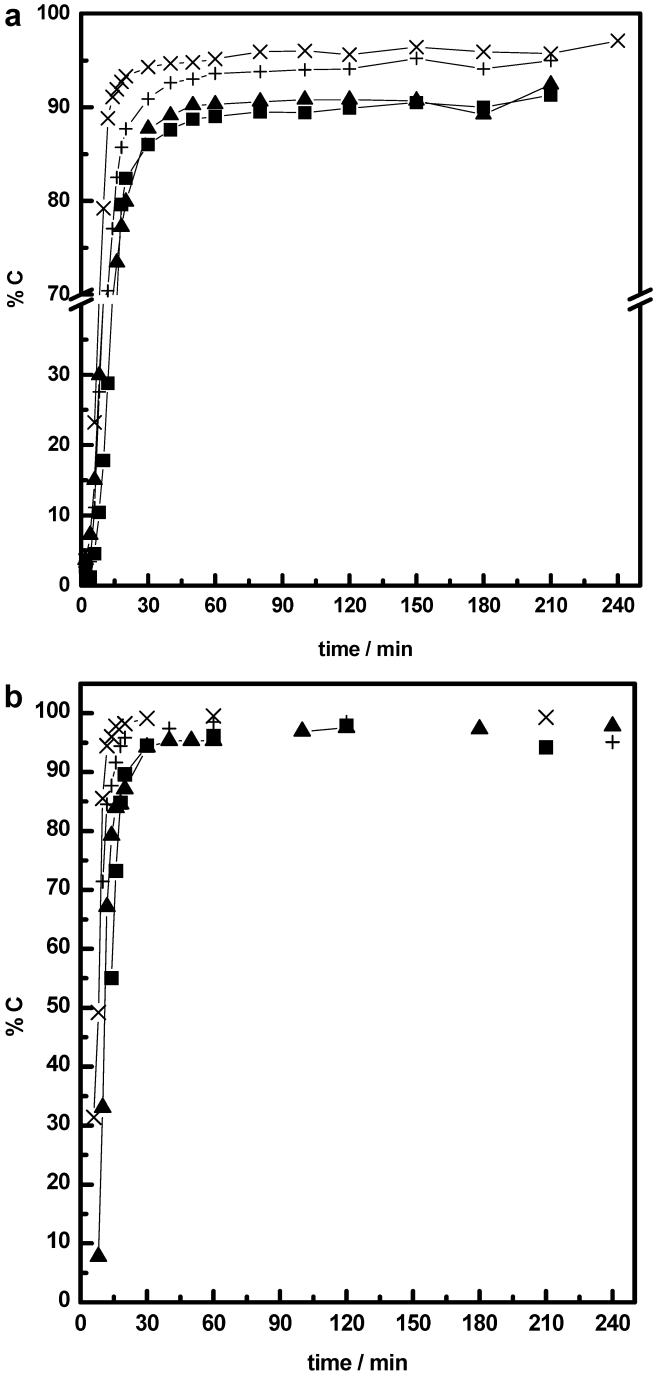

Fig. 1a,b % Conversion versus polymerization time for the MMA emulsion polymerizations of pmma§1 (■), pmma§2, 3 (▲), pmma§4 (+) and pmma§5(×). The conversion was obtained by gravimetry (**a**) and gas chromatography (**b**)

$N_p \propto [SDS]^{0.98}$. The exponent 0.98 is higher than the values found for hydrophobic monomers such as styrene [16], whose values were summarized by Fitch et al. [17]. For the emulsion polymerization of MMA in the presence of SDS, values of 3, 3.87 and 1.08 were obtained by

Table 4 Particle number density (N_p), overall rate of polymerization (R_p), average number of radicals per particle ($\bar{n}$), diameter (D_p) and polydispersity index (I_p) for pmma§1–5 latexes

Latex	D_p / (nm)	I_p	N_p /(10^{16} L^{-1})	R_p/(10^{-3} M .s^{-1})	$\bar{n}$
pmma§1	116	0.015	7.5	1.3	13
pmma§2	114	0.017	8.4	1.1	9
pmma§3	103	0.022	–	1.2	–
pmma§4	89	0.022	17.9	1.5	6
pmma§5	82	0.001	23.7	2.0	6

using potassium persulphate, Fenton's reagent and the persulphate/bisulphite/iron(II) redox system as initiator, respectively [17]. The discrepancy in the exponents may be attributed to differences in both the surfactant concentration and the experimental conditions.

Latex characterization

Particle size and size distribution

The PMMA latex particles are spherical and very narrowly size distributed as shown by the scanning electron microscopy (SEM) images (Fig. 4). The hydrodynamic particle diameter (D_p) and polydispersity index (I_p) of the latexes obtained by dynamic light scattering are collected in Table 4. The small polydispersity indexes obtained by these two techniques suggest that nucleation is fast compared to particle growth, and also the absence of a secondary nucleation step.

Electrokinetic behaviour

Figure 5 shows the electrophoretic mobility of the latex dispersions as a function of pH. For all the range of pH values the particles are negatively charged. This was expected for pH > 4.5 due to the dissociation of the surface carboxylic acid groups. The data for pmma§1 and pmma§3 samples indeed suggest the presence of carboxylic groups, which is not so obvious for pmma§4 and pmma§5. However, the negative charge at lower pH probably could also originate from some SDS molecules that remained strongly (physically and/or chemically) anchored at the polymer particle surface. The presence of these strong acid groups would more or less screen the presence of COOH groups.

The zeta potentials (ζ) were calculated from the maximum electrophoretic mobilities (μ_e) using the Helmholtz–Smoluchowski equation [18],

$$\mu_e = \varepsilon\zeta/\eta \tag{6}$$

where ε is the permittivity and η the viscosity of the medium ($\eta = 0.89$ cP at 25 °C). The surface potential (Ψ_0) and the shear plane position (Δ) were calculated from the Eversole and Boardman equation [19],

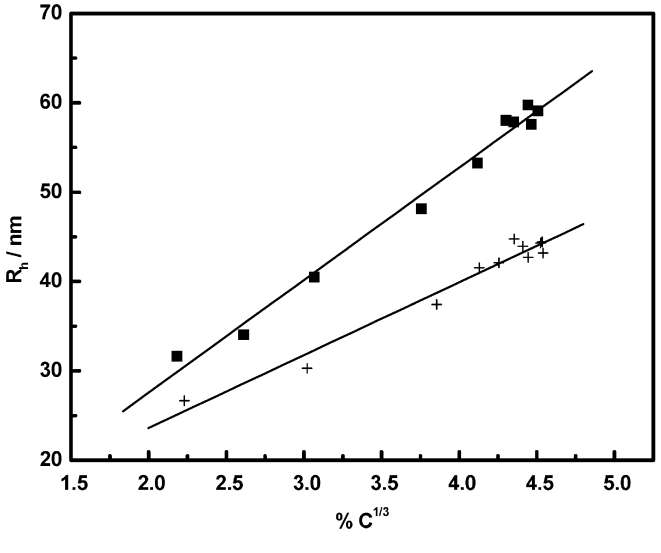

Fig. 2 Variation of R_h vs $\%C^{1/3}$ for pmma§1(■) and pmma§4 (+). The $\%C$ was obtained by gravimetry

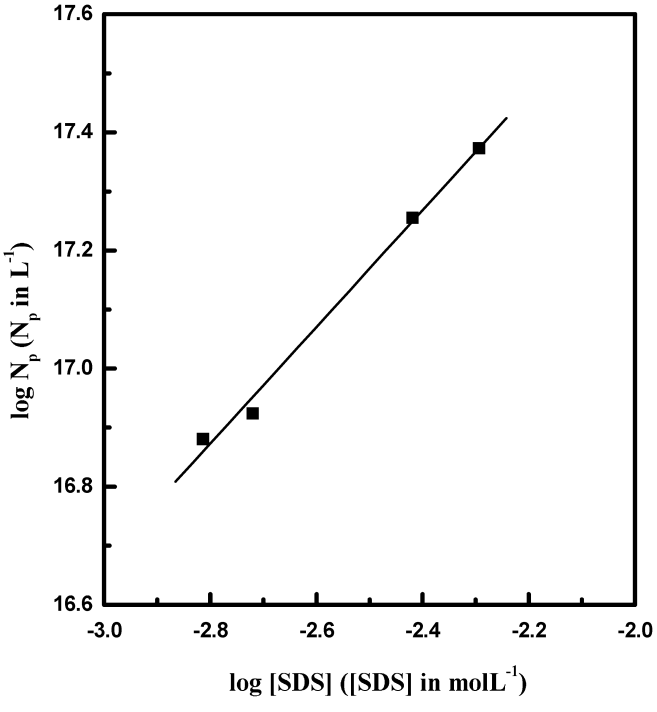

Fig. 3 Log–log plot of N_p as a function of the SDS concentration

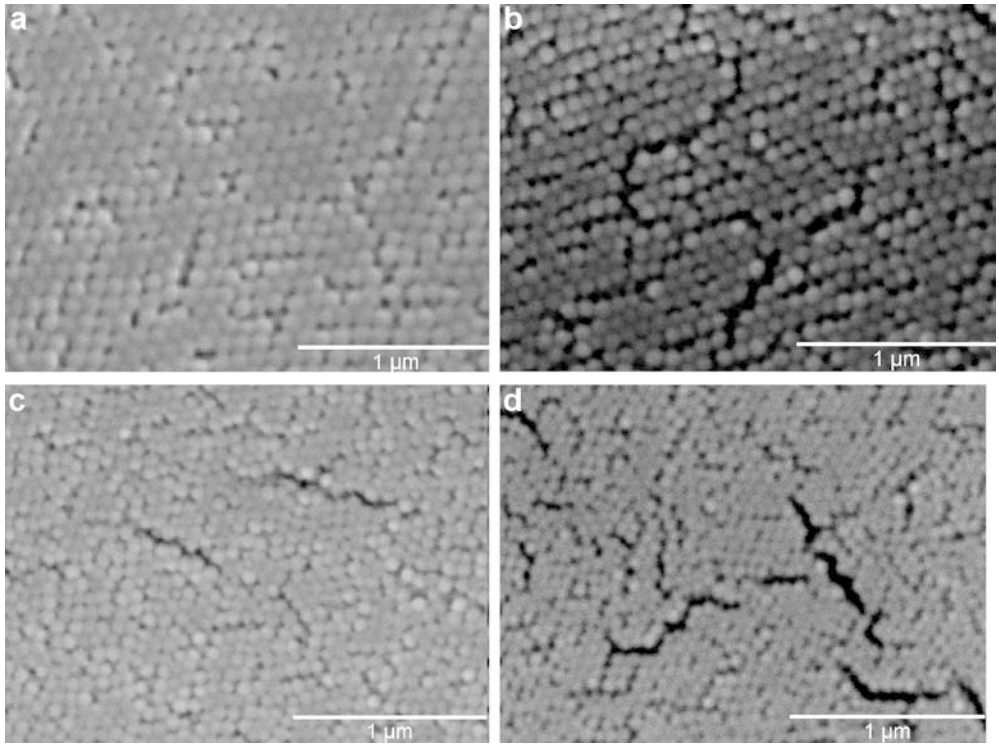

Fig. 4a–d Scanning electron microscopy images of the nanospheres: pmma§1(**a**), pmma§3 (**b**), pmma§4 (**c**) and pmma§5(**d**)

$$\ln\left(\tanh\left(\frac{e\zeta}{4kT}\right)\right) = \ln\left(\tanh\left(\frac{e\Psi_0}{4kT}\right)\right) - \kappa\Delta \qquad (7)$$

where e is the electron charge, k the Boltzmann constant, T the absolute temperature and κ the reciprocal Debye length. The values of κ (m^{-1}) were calculated by $\kappa = 3.289\times10^{9} C_s^{1/2}$, where C_s is the concentration of NaCl in mol L^{-1} [20]. Figure 6 shows the plot of $-\ln\left(\tanh\left(\frac{e\zeta}{4kT}\right)\right)$ versus κ. The linear regression allows the determination of Ψ_0 and Δ from the intercept and slope, respectively. The deviation from a straight line at low ionic strengths was already observed in other systems, being attributed to the surface conductance and/or the presence of a hairy layer interface in the particles [21]. In the present case, the thickness of the shear layer, Δ, is within 10–14 Å and the surface potential, Ψ_0, varies between −74 and −95 mV. The small thickness of the shear layer indicates the absence of a hairy layer interface.

The latex surface charge density in the shear plane, σ_e, was estimated for a 1 mM NaCl solution (pH∼10), using the approximate Eq. 8, valid for low potentials and plane interfaces.

$$\sigma_e = \mu_e \eta \kappa \qquad (8)$$

The surface charge density in the shear plane, σ_ζ, was also calculated from the more elaborate Helmholtz and Gouy–Chapman equation [22], valid for higher potentials and spherical interfaces,

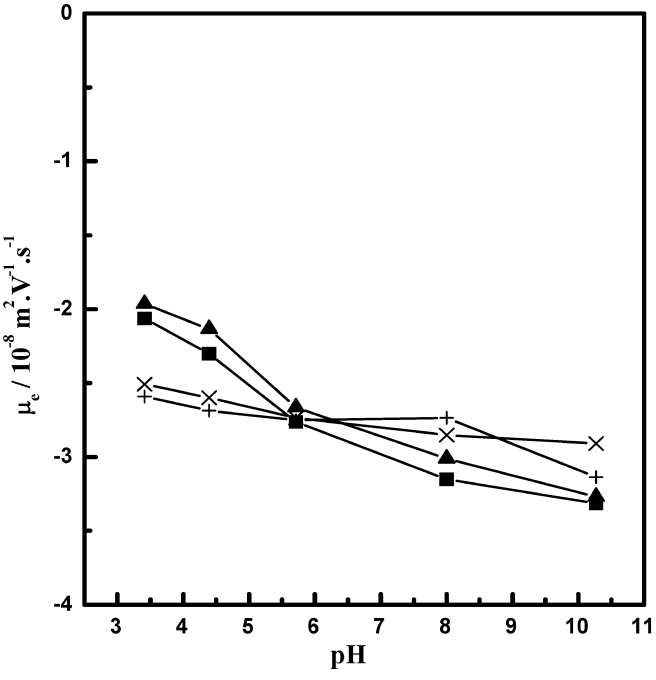

Fig. 5 Electrophoretic mobilities (μ_e) of pmma§1 (■), pmma§3 (▲), pmma§4 (+) and pmma§5(×) latex dispersions at various pH values ([NaCl] = 10^{-3} M)

$$\sigma_\zeta = \left(\frac{\varepsilon nkT}{Ze}\right)\left[2\sinh\left(\frac{Ze\Psi_0}{2kT}\right) + \frac{4}{\kappa R}\tanh\left(\frac{Ze\Psi_0}{4kT}\right)\right] \qquad (9)$$

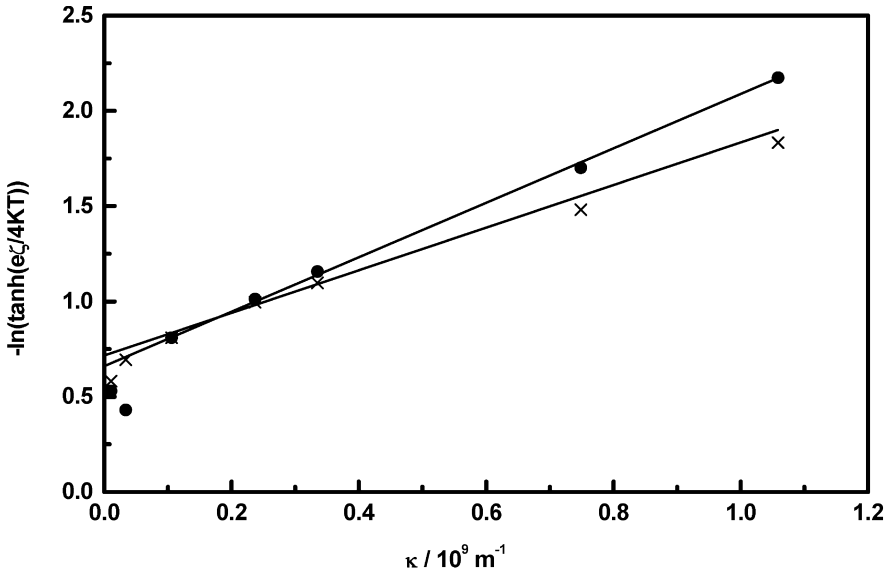

Fig. 6 $-\ln\left(\tanh\left(\frac{e\zeta}{4kT}\right)\right)$ versus κ for pmma§2 (●) and pmma§5(×) latex dispersions

where n is the electrolyte concentration expressed in ion/m^3, Z the electrolyte charge and R the particle radius.

The surface charge densities were obtained in basic solutions to guarantee that all the carboxylic groups at the surface were completely dissociated. Table 5 shows the values of σ_e and σ_ζ. The values agree reasonably well and are almost independent of the SDS concentration. The small values of the surface charge density are characteristic of latex particles bearing charges coming exclusively from the initiator.

Colloidal stability

The colloidal stability of the cleaned latexes was studied by turbidimetry at several pH and ionic strength values [23]. From the variation of the turbidity curves with time the apparent coagulation rate constants, k_{coag}, were calculated using Eq. 3. Fig. 7 shows the variation of log k_{coag} versus pH (10^{-2} M NaCl) for pmma§1 and pmma§3 latex dispersions.

Two regions can be distinguished, one below and another above the $pK_a = 4.5$ of the carboxylic acid. For $pH < 4.5$ the aggregation rate constant is pH independent, while for $pH > 4.5$, it decreases very rapidly with pH. This is in agreement with the small surface charge density, especially at $pH < 4.5$, because of the partial dissociation of the carboxylic acid groups, whereas it substantially increases for $pH > pK_a$.

The colloidal stability was then investigated as a function of ionic strength ($pH = 6$) by determining the stability factor (W) from Eq. 4. The fast coagulation rate constant was calculated from Eq. 3 at high ionic strength (0.07–0.08 M NaCl), when the charges are screened. The slow rate constants were obtained also by Eq. 3 for several solutions with lower ionic strengths. Fig. 8 shows a log–log plot of the stability factor (W) as a function of the NaCl concentration (pH∼6) for pmma§4 and pmma§5 dispersions.

Values of $W \geq 1$ correspond to stable dispersions with slow coagulation rates, whereas values of $W \sim 1$ designate unstable dispersions where fast coagulation occurs. The critical coagulation concentration (CCC) can be obtained from the stability plots (see Fig. 8), as the ionic concentration at which the two lines drawn through the experimental points of the two regions intersect. Table 6 shows the CCCs for the pmma§1, 4

Table 5 Maximum electrophoretic mobility (μ_e), zeta potential (ζ), surface potential (Ψ_0), shear plane position (Δ) and electrokinetic charge densities, σ_e and σ_ζ, for pmma§1–5 latexes

Latex	μ_e (10^{-8} m^{2}V^{-1}s^{-1})[a]	ζ/ (mV)	Ψ_0/ (mV)	Δ /(Å)	σ_e/(μC cm^{-2})	σ_ζ / (μC cm^{-2})
pmma§1	−3.32 ± 0.02	−42.2 ± 0.3	−81.7	12.0	−0.307	−0.37
pmma§2	N.D.[b]	N.D.	-83.1	14.1	N.D	N.D
pmma§3	−3.27 ± 0.02	−41.6 ± 0.3	−92.6	13.7	−0.303	−0.37
pmma§4	−3.14 ± 0.05	−39.9 ± 0.6	−74.0	14.2	−0.290	−0.36
pmma§5	−2.91 ± 0.08	−37.0 ± 1.0	−94.6	10.4	−0.269	−0.34

[a]At basic pH and 10^{-3} M NaCl concentration
[b]N.D. Not determined

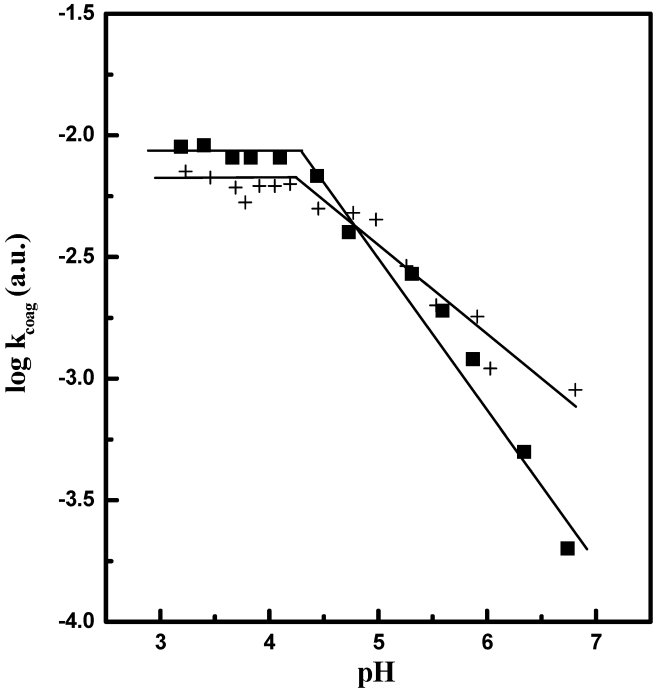

Fig. 7 log k_{coag} as a function of pH for pmma§1 (■) and pmma§3 (+) dispersions ([NaCl] = 10^{-2} M)

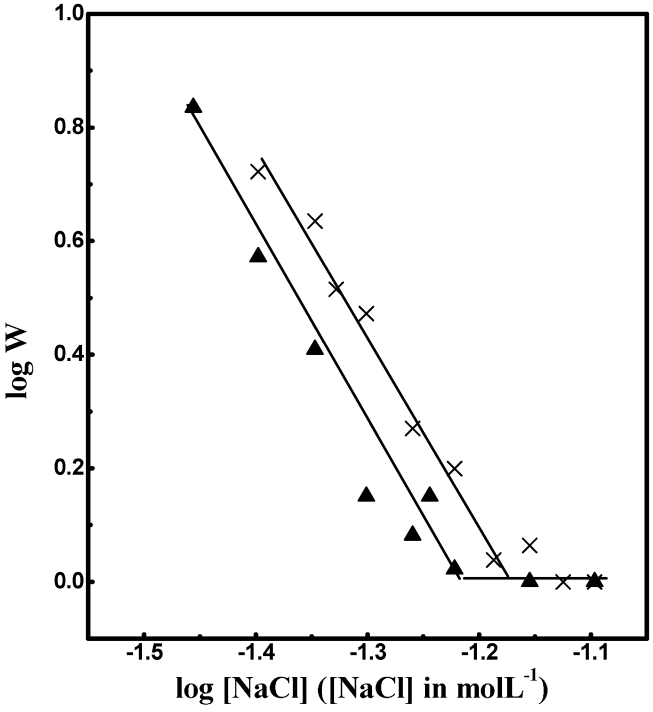

Fig. 8 Log–log plot of the stability factor (W) as a function of the electrolyte (NaCl) concentration for pmma§4 (▲) and pmma§5 (×) dispersions (pH 6)

and 5 latex dispersions. The CCC values are small due to the electrostatic stabilization of the latexes, which agrees with the low surface charge densities. CCCs around 0.1–0.2 M were reported for anionic or cationic polystyrene latexes at 20 °C [24, 25] and higher values are found when steric stabilization exists [26].

Considering the latexes as rigid spheres, an approximated relationship developed by Reerink and Overbeek [27] from the DLVO theory [28] can be used to estimate the Stern potential, Ψ_δ, from the variation of the stability factor, W, with the salt concentration, C_s. This is expressed by Eqs. 10 and 11 where γ is the surface potential function [29] and R_h the particle radius.

$$-\frac{d\ \log(W)}{d\ \log(C_S)} = 2.06 \times 10^9 \frac{R_h \gamma^2}{Z^2} \tag{10}$$

$$\gamma = \frac{\exp\left(Ze\Psi_\delta/2kT\right) - 1}{\exp\left(Ze\Psi_\delta/2kT\right) + 1} \tag{11}$$

Furthermore, the composite Hamaker constant (A_{121}) can be estimated from the critical coagulation concentration (CCC), determined from the stability plots, using Eq. 12 [29],

$$\mathrm{CCC} = \frac{9.85 \times 10^4 \varepsilon^3 k^5 T^5 \gamma^4}{N_A e^6 A_{121}^2 Z^6} \tag{12}$$

Table 6 Stern potential (Ψ_δ), critical coagulation concentration (CCC) and composite Hamaker constant (A_{121}) for pmma§1, 4 and 5 latexes

Latex	CCC / (mol L^{-1})	Slope	Ψ_δ/ (mV)	A_{121}/ (10^{-20} J)
pmma§1	0.058	N.D.[a]	N.D.	N.D.
pmma§4	0.060	−4.3	22.6	1.18
pmma§5	0.066	−3.4	20.8	0.96

[a]N.D. Not determined

where N_A is the Avogadro number.

Table 6 also shows the $\Psi_\delta$and A_{121} values for pmma§4 and 5 latexes, calculated from Eqs. 11 and 12, respectively. The Stern potential values, Ψ_δ, are very low reflecting the small charge density. The A_{121} values are in good agreement with those calculated for poly(methyl methacrylate) ($A_{121} \sim 1.05 \times 10^{-20}$ J) and polystyrene ($A_{121} \sim 0.95 \times 10^{-20}$ J) in water [30].

Conclusions

Monodisperse PMMA latex particles with small size (80–120 nm diameter) bearing carboxylic acid groups at the surface were prepared by emulsion polymerization using 4,4′-azobis(4-cyanopentanoic) acid as initiator and

sodium dodecyl sulphate as surfactant. The particle size, size distribution and surface charge density were controlled by changing the SDS concentration. Polymerization rate and particle number density increased with surfactant concentration (with an order dependency near 1.0 within the investigated concentration range) while the average particle size decreased. The maximum electrophoretic mobilities at basic pH and deduced surface charge densities were found to slightly decrease with increasing SDS concentration. Coagulation studies featured an exclusive electrostatic stability mechanism, the smaller values of the CCC compared with latexes bearing sulphate groups indicating that the carboxylic groups provided a lower stabilizing efficiency. These PMMA colloids are being applied as supports for an enzyme (cutinase) and the results on the adsorption isotherms and immobilization have already been published [31].

Acknowledgements This work was supported by the ''Fundação para a Ciência e a Tecnologia'' (FCT), Portugal, under project POCTI/33866/QUI/2000 and by Luso-French Scientific and Technical Cooperation Program. A. Santos acknowledges a PhD grant from FCT (SFRH/BD/1227/2000). The authors would like to thank Dr. Isabel Nogueira from ICEMS, IST, Lisboa for the SEM images.

References

1. Moghimi SM, Hunter AC, Murray JC (2001) Pharmacol Rev 53:283
2. Duru PE, Bektas S, Genç Ö, Patir S, Denizli A (2001) J Appl Polym Sci 81:197
3. Williamson B, Lukas R, Winnik MA, Croucher MD (1987) J Colloid Interface Sci 119(2):559
4. Bulmus V, Ayhan H, Piskin E (1997) Chem Eng J 65:71
5. Tse AS, Wu Z, Asher SA (1995) Macromolecules 28:6533
6. Ahmad H, Rahman MS, Miah MAJ, Ali AMI (2001) Colloid Polym Sci 279:1039
7. Ming W, Jones FN, Fu S (1998) Polym Bull 40:749
8. Arshady R (1999) Manufacturing methodology of microspheres. In: Arshady R (ed) Microspheres, microcapsules and liposomes. Citus, pp 85–124
9. Blackley DD (1983) Production of carboxylated latices by emulsion polymerization. In: Poehlein GW, Ottewill RH, Goodwin JW (eds) Science and technology of polymer colloids: preparation and reaction engineering, vol 1. Martinus Nijhoff, The Hague, p 203
10. Sonntag S, Strenge K (1987) Coagulation kinetics and structure formation, Plenum, New York
11. Emelie B, Pichot C, Guillot J (1985) Makromol Chem Suppl 10/11:43
12. Ozdeger E, Sudol ED, El-Aasser MS, Klein A (1997) J Polym Sci 35:3813
13. Gilbert RG (1995) Emulsion polymerization, a mechanistic approach. Academic, London
14. El-Aasser MS, Sudol ED (1997). In: Lovell PA, El-Aasser MS (eds) Emulsion polymerization and emulsion polymers. Wiley, Chichester
15. Van Herk AM (1997) Particle growth in emulsion polymerization. In: Asua JM (ed) Polymeric dispersions: principles and applications, vol 335. NATO ASI series
16. Smith WV, Ewart RH (1948) J Chem Phys 16:592
17. Fitch RM (1973) Br Polym J 5:467
18. Von Smoluchowski (1903) Bull Akad Sci Bracovie Classe Sci Math Natur 1:182
19. Hunter RJ (1981) Zeta potential in colloid science. Academic, London
20. Hiemenz PC, Rajagopalan R (1997) Principles of colloid and surface chemistry, 3rd edn. Marcel Dekker, New York
21. Folkersma R, van Diemen AJG, Stein HS (1998) Langmuir 14(21):5973
22. Russel WB, Saville DA, Schowalter WR (1989) Colloidal dispersion. Cambridge University Press
23. Prieve DC, Ruckenstein E (1980) J Colloid Interface Sci 73 (2):539
24. Graillat C, Dumont B, Depraetere P, Vintenon V, Pichot C (1991) Langmuir 7:872
25. Barbero AF, Rodriguez AM, Fernandez JC, Alvarez RH (1994) J Colloid Interface Sci 162:257
26. Duracher D, Sauzedde F, Elaissari A, Pichot C, Nabzar L (1998) Colloid Polym Sci 276:920
27. Wiersema PH, Loeb AL, Overbeek JTG (1966) J Colloid Interface Sci 22:78
28. Fitch RM (1997) Polymer colloids. Academic, London
29. Shaw DJ (1992) Introduction to colloid and surface chemistry. Butterworths, London
30. Ottewill RH (1997) Stability of polymer colloids. In: Asua JM (ed) Polymeric dispersions: principles and applications, vol 335. NATO ASI series
31. Baptista RP, Santos AM, Fedorov A, Martinho JMG, Pichot C, Elaissari A, Cabral JMS, Taipa MA (2003) J Biotechnol 102:241